Table II. MuLV production following SV40 infection of MuLV-producing cells

	MuLV-producing cells				SV40-infected MuLV-producing cells			
Passage in vitro	MuLV-specific fluorescence	Interference units per 60 mm dish	Cells per 60 mm dish	Interference units per cell	MuLV-specific fluorescence	Interference units per 60 mm dish	Cells per 60 mm dish	Interference units per cell
2	+	10^6	2×10^6	0.5				
7	+	10^5	6×10^5	0.2				
10	+	10^6	1.2×10^6	0.8	+	10^3	1.5×10^6	0.001
14	+	n.d.[a]	n.d.	n.d.	+	10^3	1.5×10^6	0.001

[a] n.d., not determined.

The sources of wild-type SV40 and MSV (Moloney) have been described[1,6]. Moloney leukaemia virus was obtained from Dr. R. J. HUEBNER as infectious tissue culture fluids. The virus was subsequently passaged in mouse embryo cells and infectious 24 h culture fluids were stored at −70 °C.

Moloney leukaemia virus was assayed by interference[5] with MSV (Moloney). Tissue culture fluids from MuLV-infected cultures were inoculated onto BALB/c primary cultures at dilutions ranging down to 10^{-6}. After 21 days incubation the cells were trypsinized and challenged by infection with MSV. Duplicate cultures were inspected 3 days later for evidence of MSV transformation. An interference unit is defined as the greatest dilution of infected tissue culture fluids able to prevent MSV transformation.

Anti-MuLV antiserum prepared in C57BL mice (by Dr. J. MOLONEY) was used in a sandwich technique with fluorescein-conjugated rabbit anti-mouse IgG. Simian virus 40 nuclear T antigen was detected with a fluorescein-conjugated antiserum produced in hamsters bearing an SV40-induced tumour (Microbiological Associates).

Results and discussion. Mouse cells have been previously shown to undergo senescence in vitro[4]. In this report, a similar curtailment of division is demonstrated in MuLV-infected cells by passages 6–7 (Table I). Although control cells remained quiescent up to passage 14, cells infected with MuLV recommenced growth as an established line by passages 9–12. The introduction of SV40 to uninfected senescent cultures resulted in even more rapid cell division and emergence of permanent cell lines. Superinfection by SV40 of an MuLV-producing line failed to enhance their growth to the same extent, although T antigen fluorescence was detected in their nuclei. Table II shows that MuLV production remained almost constant throughout the in vitro life-span of MuLV-infected cells but SV40 infection caused a marked reduction in MuLV output.

The fact that MuLV-producing cells continue extruding virus during senescence contrasts with the failure of MSV to productively infect cells already in senescence[2]. This confirms that senescent cells, once infected, are capable of supporting RNA tumour virus replication, without further cell division.

The decline in production of MuLV after infection with SV40 virus is at variance with other reports. SIMONS[7] showed that cells infected with both MSV and SV40 grew rapidly, assumed an MSV-transformed morphology and liberated increased amounts of MSV into the culture medium. Neither has interference been demonstrated between SV40 and RNA tumour viruses in other cell systems[8–10].

1 R. S. U. BAKER, P. J. SIMONS and B. J. RANKIN, J. gen. Virol. *14*, 115 (1972).
2 R. S. U. BAKER and P. J. SIMONS, J. gen. Virol. *12*, 95 (1971).
3 B. M. BUCK and R. BATHER, J. gen. Virol. *4*, 457 (1969).
4 A. A. TUFFERY and R. S. U. BAKER, Expl Cell Res. *76*, 186 (1973).
5 P. S. SARMA, M. P. CHEONG, J. W. HARTLEY and R. J. HUEBNER, Virology *33*, 180 (1967).
6 P. J. SIMONS, S. S. PEPPER and R. S. U. BAKER, Proc. Soc. exp. Biol. Med. *131*, 454 (1969).
7 P. J. SIMONS, J. gen. Virol. *19*, 411 (1973).
8 A. E. FREEMAN, G. J. KELLOFF, M. L. VERNON, W. T. LANE, W. I. CAPPS, S. D. BUMGARNER, H. C. TURNER and R. J. HUEBNER, J. natn. Cancer Inst., USA *52*, 1469 (1974).
9 J. S. RHIM, C. GREENAWALT, K. K. TAKEMOTO and R. J. HUEBNER, Nature New Biol. *230*, 81 (1971).
10 G. J. TODARO and C. A. MEYER, J. natn. Cancer Inst., USA *52*, 167 (1974).

Ultrastructure of Synapses of the Metacestode of *Hymenolepis microstoma*

R. A. WEBB*

Department of Biology, University of New Brunswick, Fredericton (N.B., Canada E3B 5A3), 26 February 1975.

Summary. The ultrastructure of the synapses of the metacestode of *Hymenolepsis microstoma* is described. Many features observed are similar to those of many invertebrate and vertebrate synapses where mechanical strength is of importance. These observations indicate an early phylogenetic origin for this type of synapse.

Numerous studies have centred on the fine structure of the nervous tissue of platyhelminths (see[1] for references). While synaptic contacts have been observed, little attention has been given to the detailed morphology of the synapse. In the present study, the numerous synapses of the metacestode of *Hymenolepis microstoma* are shown to contain many of the morphological features observed in vertebrate synapses following specialized fixation and staining techniques[2–4].

* This work was supported by a grant from the University of New Brunswick Research Fund.

1 R. A. WEBB and K. G. DAVEY, Can. J. Zool., in press (1975).
2 E. G. GRAY, Int. Rev. gen. exp. Zool. *2*, 139 (1966).
3 G. K. AGHAJANIAN and F. E. BLOOM, Brain Res. *6*, 716 (1967).
4 K. AKERT, K. PFENNINGER, C. SANDRI and H. MOORE, in *Structure and Function of Synapses* (Eds. G. D. PAPPAS and D. P. PURPURA; Raven Press, New York 1972), p. 67.

Methods. Cultures of cysticercoids of *H. microstoma* were maintained as described previously[1]. Cysticercoids were fixed in situ[5], and prepared for electron microscopy as described previously[1]. Contrasted sections were viewed in a Phillips EM 200 at 60Kv.

Results and discussion. The synaptic contacts of *H. microstoma* consist of parallel membranes of adjacent nerve processes, separated by a cleft of approximately 200 Å (Figure 1). The cleft contained material of high electron opacity. The plasma membrane, on either side of the synaptic cleft, appeared as single 60 Å lines. The membranes bounding the synaptic cleft, however, were trilaminar unit membranes, where the cytoplasmic side (inner leaflet) of each pre- and post-synaptic membrane appeared thickened (Figure 2). The trilaminar appearance of the synaptic membranes is similar to the situation observed in both Leech and Octopus synapses[6,7].

Dense projections, approximately 300×300 Å, were associated with the presynaptic inner leaflet of the plasma membrane (Figures 1 and 2). Occasionally, these pro-

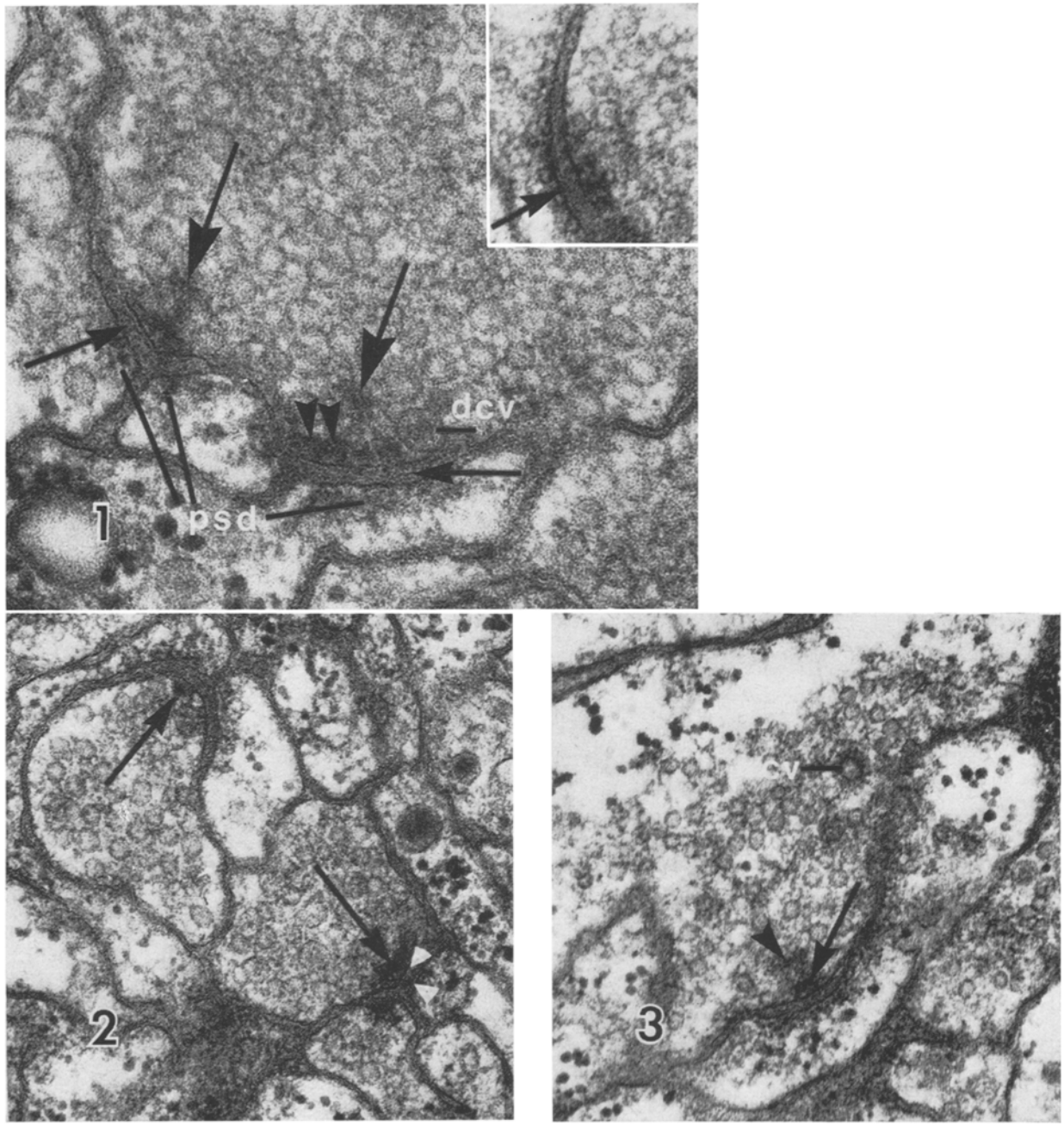

Fig. 1. Complex synaptic configuration illustrating the synaptic cleft (small arrows), the presynaptic network (large arrows) and the postsynaptic density (psd). Note the presynaptic dense projections (arrow heads) appear fused. dcv, dense cored vesicle. ×150,000. Inset. Note the trilaminar appearance of the postsynaptic membrane (arrow). ×137,000.

Fig. 2. Synaptic contacts illustrating single presynaptic dense projections (arrows) and numerous round synaptic vesicles. Note the trilaminar appearance of the synaptic membranes (arrow heads). ×83,000.

Fig. 3. Synapse showing a single presynaptic dense body (arrow), the presynaptic network (arrow head) and an adjacent complex vesicle (cv). ×79,000.

jections appeared fused. Associated with the dense projections were electron-dense strands lying deeper in the presynaptic terminal that sometimes appeared to form direct contacts with the plasma membrane. This structural aggregation, which resembled the finger-like processes observed in synapses of *Dugesia dorotocephala*[8,9], is similar to the presynaptic network of vertebrate synapses[10]. In oblique sections through the synapses of *H. microstoma*, the dense projections appeared few in number, and did not show a regular arrangement. This is in contrast to the situation observed in vertebrate synapses[4,10,11].

The presynaptic terminals were filled with numerous synaptic vesicles (200–450 Å diam.), interspersed with the occasional small dense-cored vesicles (450–750 Å diam.). Complex vesicles, from which dense projections are believed to be derived[12], were observed in the presynaptic terminal (Figure 3).

Post-synaptic densities, emanating from the inner thickened leaflet of the postsynaptic membranes (Figure 1), were a constant feature of the synapses. These structures, which were up to 300 Å wide, usually extended the length of the synaptic cleft. Whispy projections were observed, extending from the postsynaptic density into the postsynaptic space. Thus the postsynaptic densities are similar to those observed in vertebrate synapses. While the variation in width of the postsynaptic density of vertebrates is usually associated with excitatory or inhibitory synapses[4], such correlation was not possible in the present study where flattened synaptic vesicles have not been observed.

The present results therefore show that the synapses of *H. microstoma* possess almost all those features found in many higher invertebrate and vertebrate synapses, and attest to an early phylogenetic origin of this type of synapse. Several of these features, however, have not been observed in other platyhelminths or in coelenterates. For example, while small presynaptic dense projections and postsynaptic thickenings have been observed in several coelenterates[13,14], neither complex vesicles nor presynaptic networks have been described. Many of these features observed, however, may apply only to certain types of synapses where mechanical strength is of importance[15]. Such may be the case with the present material, where ,under differing experimental conditions, the extracellular space between neurites may be variable, the synaptic cleft is of constant dimensions[16]. Further research is required to allow differentiation between those structures associated with synaptic membrane adhesion, and those structures associated with chemical transmission at synapses.

[5] C. Perrachia and B. S. Mittler, J. Cell Biol. *53*, 234 (1972).
[6] E. G. Gray and R. W. Guillery, Z. Zellforsch. *60*, 826 (1963).
[7] E. G. Grey and J. Z. Young, J. Cell Biol. *21*, 87 (1964).
[8] D. G. Jones, Z. Zellforsch. *95*, 263 (1969).
[9] M. Morita and J. L. Best, J. exp. Zool. *161*, 391 (1966).
[10] D. G. Jones and R. F. Brearley, Z. Zellforsch. *125*, 415 (1972).
[11] E. G. Grey, J. Anat. *97*, 101 (1963).
[12] D. G. Jones and H. F. Bradford, Tissue Cell *3*, 177 (1971).
[13] D. J. Peteva, Z. Zellforsch. *141*, 301 (1973).
[14] J. A. Westfall, S. Yamataka and P. D. Enos, J. Cell Biol. *51*, 318 (1971).
[15] J. L. S. Cobb and P. A. Mullins, Z. Zellforsch. *138*, 75 (1973).
[16] Personal communication.

The Fine Structure of the Conical-Headed Sperm of the Crinoid *Antedon bifida*

N. D. Holland

Division of Marine Biology, Scripps Institution of Oceanography, University of California at San Diego, P.O. Box 1529, La Jolla (California 92037, USA), 25 August 1975.

Summary. Scanning- and transmission electron microscopy show that the sperm head of *Antedon bifida* is conical and thus different from the spherical sperm head that is typical of crinoids. The head consists of the acrosome and the nucleus. The posterior fibrogranular component of the acrosome is housed in a tubular, axial invagination running from the anterior pole almost to the posterior pole of the nucleus. The middle piece includes a mitochondrion and a pair of centrioles. One of the centrioles is a basal body, which gives rise to the tail flagellum.

In the echinoderm class Crinoidea, the sperm is divisible into a head, a middle piece and a tail. The sperm head is approximately spherical in many species of stalked and unstalked crinoids[1–5]. By contrast, a conical sperm head was reported for the crinoid *Antedon bifida* by Chadwick[6] in 1907. I once suspected[5] that Chadwick had mistaken a spherical head for a conical head. However, my recent electron microscopy has shown that Chadwick was correct and that I have been the mistaken one, since the sperm head of *Antedon bifida* is indeed conical. The present report describes the fine structure of sperm from ripe male specimens of *Antedon bifida* collected at Plymouth, England[7]. The methods for the scanning- and transmission electron microscopy have already been published elsewhere[8].

The scanning electron micrograph (Figure 1) shows the sperm head, the middle piece and the proximal part of the tail. The conical sperm head is 2 μm in length by 1.1 μm in maximum width. The middle piece is 0.7 μm long by 1.3 μm wide. The tail, as measured from whole mounts of freshly killed sperm, is roughly 50 μm long.

Transmission electron micrographs (Figure 2, a and b) show that the sperm head is made up of an acrosome and a nucleus. The acrosome consists of a spherical acrosomal granule and the surrounding fibrogranular material. The acrosomal granule is about 0.5 μm in diameter, and the posterior pole of the granule has a small concavity 0.05 μm deep (Figure 2b). The granule is filled with amorphous contents of moderate electron density. The fibro-granular acrosomal material outside of the granule is divided into

[1] H. Ludwig, Z. wiss. Zool. *29*, 47 (1877).
[2] D. C. Danielssen, Norske Nordhavs-Expedition 1876–1878, *5*, 1 (1892).
[3] G. Retzius, Biol. Untersuch. *12*, 79 (1905).
[4] J. C. Dan, Adv. Morphogen. *8*, 1 (1970).
[5] F. S. Chia, D. Atwood and B. Crawford, Am. Zool. *15*, 533 (1975).
[6] H. C. Chadwick, Proc. Trans. Liverpool biol. Soc. *21*, 371 (1907).
[7] Animals were collected through the cooperation of the director and staff of the Laboratory of the Marine Biological Association of the United Kingdom, Plymouth, England.
[8] N. D. Holland and Å. Jespersen, Tissue Cell *5*, 209 (1973).